*Aerosol and Air Quality Research*, 16: 464–469, 2016

ISSN: 1680-8584 print / 2071-1409 online
doi: 10.4209/aaqr.2015.02.0089

**Technical Note**

# Inexpensive Automated Atmospheric Measurements of Aerosol Optical Thickness, Ozone, and Temperature

**Mark J. Perri*, Michael R. Haggmark, Dylan R. Silva, Ross M. Mohs**

*Department of Chemistry, Sonoma State University, 1801 E. Cotati Ave, Rohnert Park, CA 94928, USA*

## ABSTRACT

An inexpensive platform has been developed for automated measurements of air quality. Low-cost sensors for aerosol optical thickness, ozone, temperature, relative humidity, and pressure were combined with a low-cost computer (Raspberry Pi) for automated monitoring. The Raspberry Pi is well-suited to automated measurements because of: (1) its low cost, (2) its low power consumption, (3) its ability to communicate over Ethernet or wireless networks and (4) its ability to interface with many sensors through analog-to-digital converters or directly through Universal Serial Bus (USB), serial port, Inter-Integrated Circuit ($I^2C$), and Serial Peripheral Interface (SPI). This setup is appropriate for use in, e.g., undergraduate atmospheric research groups, where the cost of typical automated sensors is prohibitively expensive. We report measurements taken over a two-month period which includes evidence of high nighttime ozone due to being downwind of a forest fire. This platform can be expanded to enable other atmospheric measurements from a number of sensors.

***Keywords:*** Aerosol optical thickness; Automated measurement; Undergraduate research; Raspberry Pi.

## INTRODUCTION

Atmospheric aerosols degrade air quality, are associated with adverse health effects (Poschl, 2005), and influence radiative forcing and climate (Kanakidou *et al.*, 2005; IPCC, 2007). Atmospheric models under-predict organic aerosol concentrations in the free troposphere (Heald *et al.*, 2005). Much work has focused on identifying aerosol sources, e.g., secondary organic aerosol (SOA) formation in cloud processing (Blando *et al.*, 1998; Monod *et al.*, 2005; Ervens and Kreidenweis, 2007; Nozière *et al.*, 2007; Ervens *et al.*, 2008; Lim and Ziemann, 2009; Perri *et al.*, 2009; Lim *et al.*, 2010), SOA formation on acidic seed particles (Jang *et al.*, 2002; Gao *et al.*, 2004; Iinuma *et al.*, 2004; Kleindienst *et al.*, 2006), and organosulfate formation (Maria *et al.*, 2003; Romero and Oehme, 2005; Gao *et al.*, 2006; Surratt *et al.*, 2008; Perri *et al.*, 2010). It is clear that measurements of tropospheric aerosol concentrations are of global importance.

The primary instrument used in this study is an inexpensive yet high-quality handheld sun photometer (Brooks and Mims, 2001). The GLOBE sun photometer instrument is used globally to determine Aerosol Optical Thickness (AOT) (Boersma and de Vroom, 2006); however, its measurement frequency is limited by the human interaction required. To assist in expanding the number of measurements made by this device, an automated platform has been developed. This platform automatically measures and records AOT using the GLOBE sun photometer. It also serves as an expandable hub for any number of instruments. Here we demonstrate automated AOT data collected as well as additional connections to three sensors: pressure, temperature/humidity, and ozone mixing ratio. The setup is inexpensive enough for undergraduate research labs to afford.

## METHODS

### *Atmospheric Sensors*

The full sensor system is described in detail below. A summary of sensor specification and pricing is reported in Table 1. Briefly, the system consists of: a photometer that automatically pans and tilts to face the sun (Fig. 1), a webcam to take pictures of the sun and sky, an ozone monitor, a temperature and humidity sensor, and a pressure sensor. A small computer (Raspberry Pi) interfaces with all sensors and logs the data in a file. All components run off DC power provided by AC to DC power adapters, but power could also be provided by a 12 V battery and DC-to-DC converter for field use.

The GLOBE Sun Photometer is described in detail elsewhere (Brooks and Mims, 2001). Briefly, inexpensive light emitting diodes (LEDs) are used as light sensors. In this study the red LED channel (absorption maximum at 625 nm)

* Corresponding author.
Tel.: 1-707-664-2440; Fax: 1-707-664-3378
*E-mail address:* mark.perri@sonoma.edu

**Table 1.** Sensor components, specifications, suppliers, and pricing.

| Component | Cost | Specifications | Connection Type |
|---|---|---|---|
| Raspberry Pi model B | $40 | USB, Ethernet, General Purpose IO Linux Microcomputer | |
| Sun Photometer | $140 | | ADC, 0–2 V |
| Omega Engineering Pressure Transducer MMA030V5T4A1T3A5 | $495 | 0–1500 Torr ± 0.2% | ADC, 0–5 V |
| Omega Engineering RH318 Temperature Data Logger | $299 | –20°C to 60°C ± 0.8°C<br>0 to 100% RH ± 2%<br>Resolution: 0.1°C, 0.1% RH | Serial over USB |
| Aeroqual Series 500 Ozone Monitor | $1395 | 5–150 ppb ± 5 ppb<br>Resolution: 2 ppb | ADC, 0–5 V |
| 10-bit 4-channel analog to digital converter (ADC) (Microchip MCP3004) | $2.50 | 10 bit | SPI |
| Adafruit PCA 9685 Servo Driver | $15 | 16-channel Pulse Width Modulation (PWM) | $I^2C$ |
| Hitec Servo HS-645MG (2 ea) | $31 ea | Metal Gear, 133 oz-in torque 0.20 sec/60° | |
| Servo City SPT200H Pan and Tilt System | $46 | | |
| Total Cost | $2495 | | |

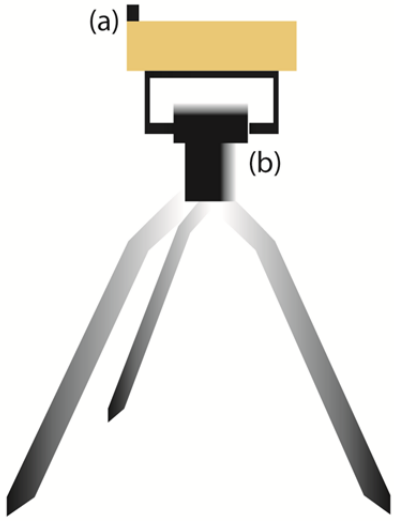


**Fig. 1**. GLOBE Sun Photometer setup: (a) photometer and (b) two servos with pan and tilt mount. Not shown: small rack to hold the ozone, temperature, and pressure sensors along with Raspberry Pi and wiring.

was monitored. The LED sensor is located inside a plastic box and aligned with a small aperture that serves as an optical baffle, so that only direct sunlight is measured. The current generated when photons strike the LED is converted to a voltage and amplified using an operational amplifier, providing a voltage output that varies between 4 mV in darkness to approximately 1.8 V in full sun.

The photometer was mounted on a pan and tilt system marketed for camera manipulation (SPT200H, Servo City). The pan and tilt setup was machined to hold the photometer and fitted with two servo motors (HiTEC HS-645 Metal Gear High Torque Servo). The servo motors are controlled by a 12-bit 16-channel Pulse Width Modulation (PWM) Inter-Integrated Circuit (I2C) interface board (Adafruit PCA 9685). Sensor data from the photometer is read via a 10-bit 4-channel analog to digital converter (ADC) (Microchip MCP3004) over the Serial Peripheral Interface (SPI).

The Raspberry Pi is a miniature-sized (86 mm × 56 mm × 21 mm) but full computer running linux with integrated Ethernet communication. It is ideal for field deployment because it runs off 5 VDC and only requires 2 W of power. The Raspberry Pi exposes several general purpose input and output (GPIO) pins. These GPIO pins are used to directly interface with the sensors used in this section via $I^2C$, SPI, serial communications, and USB. A circuit diagram of the Raspberry Pi connections to the sensors, servo controller, and power supply is given in the Supplemental Information (Fig. SI-1). The Ethernet connection regularly uploads data to a file server. A python program on the Raspberry Pi controls communication with the $I^2C$ servo controller to position the photometer so that the LED sensor has direct line of sight to the sun and logs the analog sensor output to a file. The position (azimuth and angle) of the sun are calculated using the python library, pysolar (Stafford, 2013), and the Raspberry Pi converts the desired angle into servo positions and sends appropriate commands to the servo controller. Data is collected every 8 minutes.

The photometer was set on the roof (15 m height) of the Darwin Science and Technology building in the Sonoma State Campus (Rohnert Park, CA) facing south. Using the pan and tilt setup, a servo control pulse of 160 ms rotates the photometer 96° to the left (facing east) and a pulse of 680 ms rotates 96° to the right (facing west). The tilt servo receives control pulses between 410 ms (8° elevation below the horizon) to 210 ms (71° elevation above the horizon). Pictures of the sun and surrounding sky were taken using a webcam mounted on top of the photometer (Logitech C310),

connected via USB to the Raspberry Pi. After acquiring a photometer reading the camera records a direct picture of the sun and then creates a panoramic photo of the entire sky in order to record the sun position relative to any interfering clouds.

Ground-level ozone mixing ratio was measured by an Aeroqual Series 500 ultra-low ozone monitor with the following specifications: 5–150 ppb range; ± 5 ppb accuracy; 2 ppb resolution (Aeroqual, 2011). This is a handheld ozone monitor that incorporates a small sampling fan to draw air over the sensor head. This economical sensor head uses a proprietary gas sensitive semiconductor (GSS) that is interchangeable with other Aeroqual sensor heads (e.g., CO, VOC, and $SO_2$). The ozone monitor's analog output was logged by the Raspberry Pi using the ADC mentioned above. Pressure was measured by a transducer (MMA030V5T4A1T3A5, Omega Engineering) whose analog output was read using the ADC. Temperature, humidity, and dew point were measured by an RH318 (Omega Engineering) Temperature Data Logger, which communicates with the Raspberry Pi via serial pins on the GPIO header. The instrument prototype is not weatherproof. All sensors plus the Raspberry Pi were located in a small homemade rack (approximately 0.3 m × 0.3 m × 0.3 m). The instrument rack was placed on the rooftop and an effort was made to expose the sensors as best as possible to ambient air. The Raspberry Pi monitored the National Weather Service's forecast (National Oceanic and Atmospheric Administration, 2013) and emailed the researchers if a chance of rain was detected. The instrument was taken inside to protect it from rain, resulting in data gaps.

### *Data Processing*

Aerosol optical thickness (AOT) was calculated from the photometer analog output based on the photometer reading, the extraterrestrial constant $V_o$ (provided by the manufacturer), the solar zenith angle, and pressure (Brooks and Mims, 2001; Brooks, 2013). AOT must be corrected for the temperature dependence of the electronics, most notably the LED and op-amp (Brooks and Mims, 2001). Typically a GLOBE sun photometer is stored inside and only brought out for measurements. Because this photometer was deployed outside in this study its internal temperature varied from 5°C to 40°C throughout the day. The temperature dependence of the photometer output was experimentally determined using an external lamp source (Kodak AF-3 slide projector). The photometer was cooled to 0°C in a –20°C freezer, then placed in front of the slide projector and heated with a laboratory heat gun. The internal temperature and the photometer output voltage were measured between 0°C to 35°C and the mean temperature dependence was found to be 0.004 V/°C ($\sigma$ = 0.002; N = 13). All voltage readings were corrected based on the temperature data logger reading to a temperature of 22.5°C (the suggested operating temperature of the photometer is 20°C–25°C). It is clear that a diurnal variation in AOT was still present after temperature correction, likely due to a difference in the temperature internal to the photometer (in full sun) and the temperature data logger sensor (in shade). This illustrates that temperature measurement inside the photometer itself during measurements would be beneficial.

Absorption from ozone results in an increase in measured optical thickness of 0.031 AOT per 300 Dobson Units total column ozone (Brooks, 2013). Total column ozone was not measured in this study, so an approximate correction assuming a 300 Dobson Unit total column was used based on the average of data from the Ozone Monitoring Instrument (OMI) satellite (Ziemke *et al.*, 2006) for the local area. Daily total column ozone fluctuations on the order of 10% will therefore produce an error of 0.003 AOT, or 2% of an average reading of 0.14 AOT. Errors arising from seasonal variations in total column ozone on the order of 20% could be reduced by periodic adjustments based on satellite data.

The analog output was filtered for cloud influence. Photometer outputs below 0.1 V were automatically discarded (valid readings varied between 0.3 V at sunrise/sunset to 1.8 V at midday). Scattered clouds interfered with many morning measurements and were filtered by the computer by comparing subsequent measurements and removing measurements that are too far from previous measurements. The user also validated and/or overrode the automatic cloud filtering by viewing pictures taken from a webcam located on top of the photometer.

## RESULTS AND DISCUSSION

Rohnert Park, CA lies 50 miles NW of San Francisco, CA and has a population of 40,971 (U.S. Census Bureau, 2010). In general the air in Rohnert Park is quite clean; AOT, ozone mixing ratio, and temperature are shown in Fig. 2. Overall, AOT measurements averaged 0.14 over the recorded period (September 2013); ozone mixing ratio averaged 21.6 ppb between 6 am and 8 pm, usually dropping below 5 ppb at night. Skies are typically cloudy from sunrise to 9 am and then clear until sunset. We focus on two periods during this study. First, the hottest days generally corresponded with the highest ozone recorded; see for example, September 6 and 7 (Julian date 249 and 250; maximum temperatures of 41.1 and 43.6°C) with corresponding ozone mixing ratios of 40.7 and 42.8 ppb. More interesting, persistent levels of ozone, even at night were observed starting at local noon on September 10 (Julian date 253) with a corresponding AOT maximum of 0.22 during the day. This event lasted for two days. Wind trajectories (Fig. 3) from the NOAA HYSPLIT model (Draxler and Rolph, 2013) show local air originated 12–18 hours earlier near Redding, CA where an 8,073 acre forest fire broke out on the previous day at 12:30 pm local time (UTC–7). Fires are known to increase ozone and PM levels (Reid *et al.*, 2005) and the automated instrument recorded both. Other periods of non-zero nighttime ozone with corresponding high daytime AOT of 0.19 (e.g., October 11, Julian date 284) were recorded, but it is unclear what the cause was on these days. Additional sensors would aid in locating the cause and can certainly be easily interfaced with the system described here.

### *Comparison with AirNow Data*

An EPA AirNow site (San Francisco Bay Area Air Quality

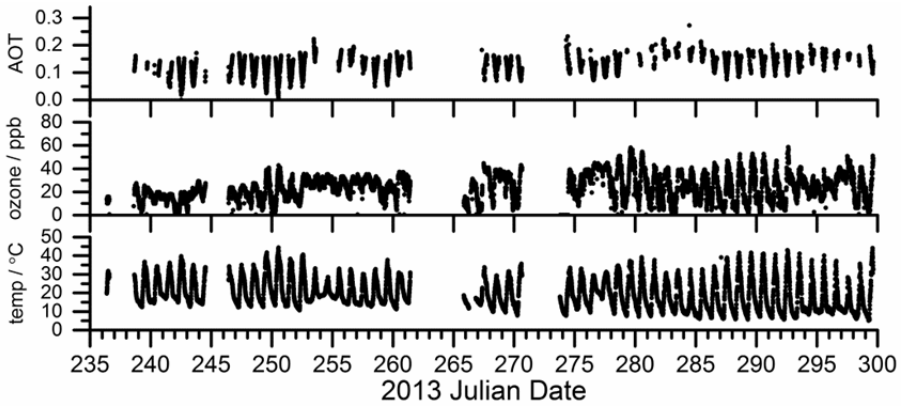


**Fig. 2.** Aerosol optical thickness (red channel) from September–October 2013. Gaps in the time series represent cloudy and/or rainy days.

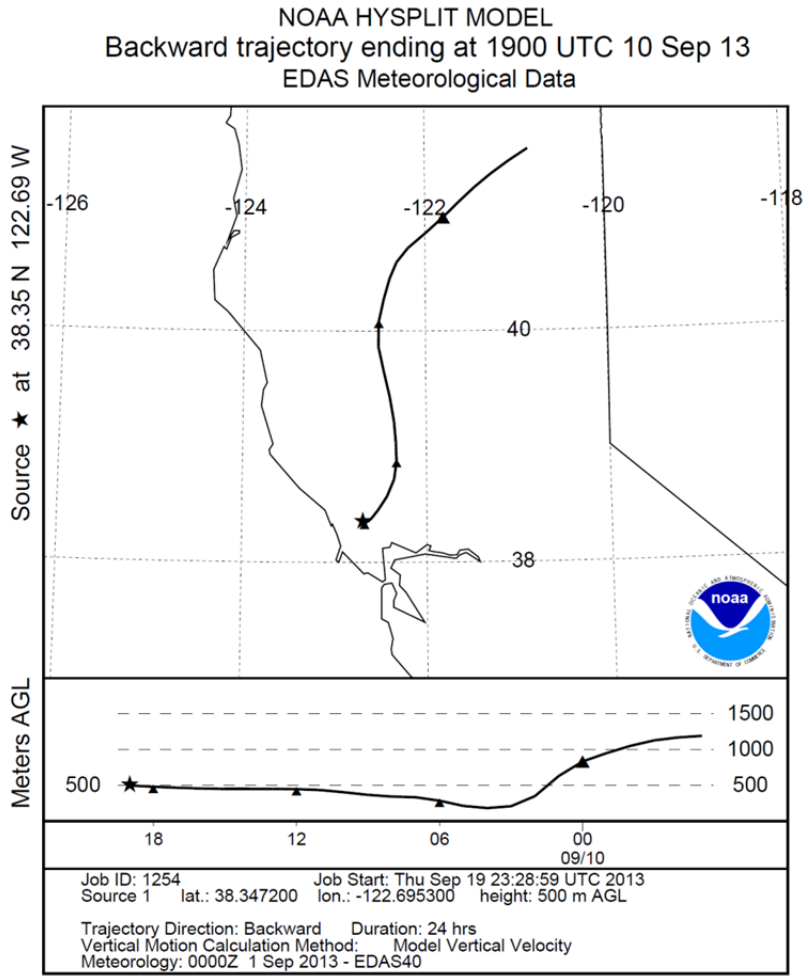


**Fig. 3.** Backward trajectory data from NOAA's HYSPLIT model showing air travel from a forest fire to the instrument's location.

Management District, 2013) is located in Santa Rosa, CA, 7.4 miles NNW of this site. The AirNow site records hourly ozone and $PM_{2.5}$ data. Ozone data from this study (SSU data) was averaged hourly and overlaid with ozone data from the Santa Rosa site (AirNow data) (Fig. 4). The two data sets are qualitatively similar and show the same trends with time. There are however quantitative differences in the two datasets. First, the granularity of the SSU ozone data is due to the 2 ppb resolution limitation of this study's Aeroqual ozone monitor readout (the AirNow site reports to 1 ppb resolution and its data is further smoothed by the line plot). Second, the SSU ozone measurements in this

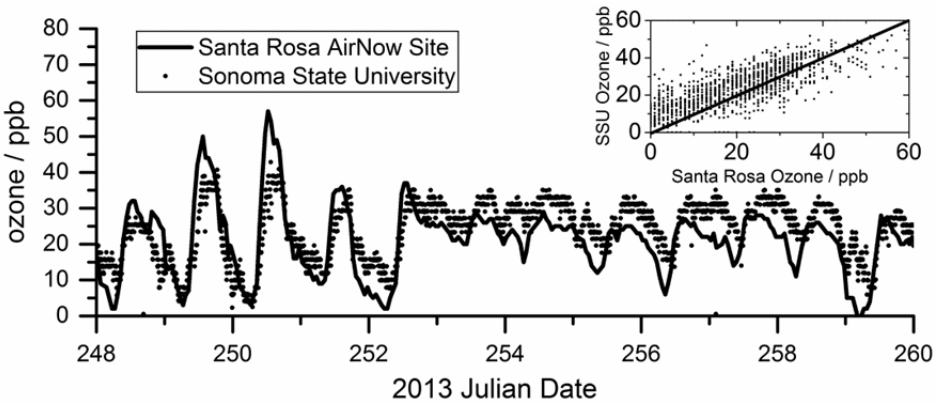


**Fig. 4.** Comparison of ozone measurements from this study (dots) with an AirNow site, 7.4 mi NNW as a function of time (main graph) and versus each other (inset, with 1:1 line drawn).

study are biased at low ozone mixing ratio, reading too high by an average of 10 ppb and also biased at high ozone mixing ratio, reading low by an equal amount (see inset, Fig. 4). A plot of the SSU ozone vs the AirNow data yields a slope of 0.7 with y-intercept of 10 ppb. The Aeroqual sensor used at the SSU site is sensitive to $NO_2$: the factory specification of this sensor is that 500 ppb of $NO_2$ will add 100 ppb to the ozone reading (Aeroqual, 2015). If VOC conditions were such that high $NO_2$ levels correspond to low ozone mixing ratios then it is reasonable that an instrumental bias due to $NO_2$ was observed at low ozone. $NO_2$ is not measured at the SSU site nor at the AirNow site so this cannot be corrected for, but future instruments could include a second sensor for this purpose. The slope of less than 1 is likely due to the geometry of the apparatus. While care was taken to expose the ozone monitor to ambient air as much as possible, it still had to be fastened to the homemade sampling rack placed directly on the rooftop. It is likely that high ozone levels were diminished by reactions with the sample rack and rooftop. Comparison of AOT from this study and $PM_{2.5}$ from the AirNow site showed little or no correlation (not shown). $PM_{10}$ was not recorded at the AirNow site, so a comparison of AOT and total PM cannot be made. Nearby AERONET sites within 100 miles (NASA Ames or McClellan AFB) do not provide aerosol data for the period of the study to compare.

## CONCLUSIONS

An inexpensive automated platform for air quality measurements has been described. Aerosol optical thickness, ozone mixing ratio, temperature, relative humidity, and pressure were recorded over a two month period from a roof-mounted device. During this time it recorded periods of high nighttime ozone and high AOT that was traced to a forest fire. This device costs significantly less ($2500 total cost) to deploy than typical instruments and is suitable for continuous monitoring in undergraduate research groups when care is taken with temperature correction and ozone monitor placement. It is easily expandable to record measurements from any instrument via analog, serial, or USB output.

## ACKNOWLEDGMENTS

This research was supported in part by grants from the Sonoma State University Research, Scholarship, and Creative Activities Program (RSCAP) and the Sonoma State Science and Technology Professional Development Fund.

## SUPPLEMENTARY MATERIAL

Supplementary data associated with this article can be found in the online version at http://www.aaqr.org.

## REFERENCES

Aeroqual (2011). Aeroqual Series 200, 300, & 500 Handheld Instruments User Guide.

Aeroqual (2015). Aeroqual Ozone Sensor Cross Sensitivity Data.

Blando, J.D., Porcja, R.J., Li, T.H., Bowman, D., Lioy, P.J., Turpin, B.J. (1998). Secondary Formation and the Smoky Mountain Organic Aerosol: An Examination of Aerosol Polarity and Functional Group Composition during SEAVS. *Environ. Sci. Technol.* 32: 604–613.

Boersma, K.F. and de Vroom, J.P. (2006). Validation of MODIS Aerosol Observations over the Netherlands with GLOBE Student Measurements. *J. Geophys. Res.* 111: D20311.

Brooks, D.R. Calculating Aerosol Optical Thickness. https://www.cs.drexel.edu/~dbrooks/globe/aot_eq.html.

Brooks, D.R. and Mims, F.M., III (2001). Development of an Inexpensive Handheld LED-based Sun Photometer for the GLOBE Program. *J. Geophys. Res.* 106: 4733–4740.

Draxler, R.R. and Rolph, G.D. (2013). HYSPLIT (HYbrid Single-Particle Lagrangian Integrated Trajectory) Model. NOAA ARL READY Website, http://www.arl.noaa.gov/HYSPLIT.php. NOAA Air Resources Laboratory, College Park, MD.

Ervens, B., Carlton, A.G., Turpin, B.J., Altieri, K.E., Kreidenweis, S.M. and Feingold, G. (2008). Secondary Organic Aerosol Yields from Cloud-processing of Isoprene Oxidation Products. *Geophys. Res. Lett.* 35: L02816.

Ervens, B., Kreidenweis, S.M. (2007). SOA formation by

biogenic and carbonyl compounds: Data evaluation and application. *Environ. Sci. Technol.* 41: 3904–3910.

Gao, S., Ng, N.L., Keywood, M., Varutbangkul, V., Bahreini, R., Nenes, A., He, J.W., Yoo, K.Y., Beauchamp, J.L., Hodyss, R.P., Flagan, R.C. and Seinfeld, J.H. (2004). Particle Phase Acidity and Oligomer Formation in Secondary Organic Aerosol. *Environ. Sci. Technol.* 38: 6582–6589.

Gao, S., Surratt, J.D., Knipping, E.M., Edgerton, E.S., Shahgholi, M. and Seinfeld, J.H. (2006). Characterization of Polar Organic Components in Fine Aerosols in the Southeastern United States: Identity, Origin, and Evolution. *J. Geophys. Res.* 111: D14314.

Heald, C.L., Jacob, D.J., Park, R.J., Russell, L.M., Huebert, B.J., Seinfeld, J.H., Liao, H. and Weber, R.J. (2005). A Large Organic Aerosol Source in the Free Troposphere Missing from Current Models. *Geophys. Res. Lett.* 32: L18809.

Iinuma, Y., Böge, O., Gnauk, T. and Herrmann, H. (2004). Aerosol-chamber Study of the Alpha-pinene/$O_3$ Reaction: Influence of Particle Acidity on Aerosol Yields and Products. *Atmos. Environ.* 38: 761–773.

IPCC (2007). Climate Change 2007: Synthesis Report. Contribution of Working Groups I, II, and III to the Fourth Assessment Report of the Intergovernmental Panel on Climate Change. Core Writing Team, Pachauri, R.K. and Reisinger, A. (Eds.), Geneva, Switzerland.

Jang, M.S., Czoschke, N.M., Lee, S. and Kamens, R.M. (2002). Heterogeneous Atmospheric Aerosol Production by Acid-catalyzed Particle-phase Reactions. *Science* 298: 814–817.

Kanakidou, M., Seinfeld, J.H., Pandis, S.N., Barnes, I., Dentener, F.J., Facchini, M.C., Van Dingenen, R., Ervens, B., Nenes, A., Nielsen, C.J., Swietlicki, E., Putaud, J.P., Balkanski, Y., Fuzzi, S., Horth, J., Moortgat, G.K., Winterhalter, R., Myhre, C.E.L., Tsigaridis, K., Vignati, E., Stephanou, E.G. and Wilson, J. (2005). Organic Aerosol and Global Climate Modelling: A Review. *Atmos. Chem. Phys.* 5: 1053–1123.

Kleindienst, T.E., Edney, E.O., Lewandowski, M., Offenberg, J.H. and Jaoui, M. (2006). Secondary Organic Carbon and Aerosol Yields from the Irradiations of Isoprene and Alpha-pinene in the Presence of $NO_x$ and $SO_2$. *Environ. Sci. Technol.* 40: 3807–3812.

Lim, Y.B. and Ziemann, P.J. (2009). Kinetics of the Heterogeneous Conversion of 1,4-hydroxycarbonyls to Cyclic Hemiacetals and Dihydrofurans on Organic Aerosol Particles. *PCCP* 11: 8029–8039.

Lim, Y.B., Tan, Y., Perri, M.J., Seitzinger, S.P. and Turpin, B.J. (2010). Aqueous Chemistry and its Role In Secondary Organic Aerosol (SOA) Formation. *Atmos. Chem. Phys.* 10: 10521–10539.

Maria, S.F., Russell, L.M., Turpin, B.J., Porcja, R.J., Campos, T.L., Weber, R.J. and Huebert, B.J. (2003). Source Signatures of Carbon Monoxide and Organic Functional Groups in Asian Pacific Regional Aerosol Characterization Experiment (ACE-Asia) Submicron Aerosol Types. *J. Geophys. Res.* 108: 8637.

Monod, A., Poulain, L., Grubert, S., Voisin, D. and Wortham, H. (2005). Kinetics of OH-initiated Oxidation of Oxygenated Organic Compounds in the Aqueous Phase: New Rate Constants, Structure–Activity Relationships and Atmospheric Implications. *Atmos. Environ.* 39: 7667–7688.

National Oceanic and Atmospheric Administration National Weather Service. forecast.weather.gov.

Nozière, B., Dziedzic, P. and Córdova, A. (2007). Formation of Secondary Light-absorbing "Fulvic-like" Oligomers: A Common Process in Aqueous and Ionic Atmospheric Particles? *Geophys. Res. Lett.* 34: L21812.

Perri, M.J., Seitzinger, S. and Turpin, B.J. (2009). Secondary Organic Aerosol Production from Aqueous Photooxidation of Glycolaldehyde: Laboratory Experiments. *Atmos. Environ.* 43: 1487–1497.

Perri, M.J., Lim, Y.B., Seitzinger, S.P. and Turpin, B.J. (2010). Organosulfates from Glycolaldehyde in Aqueous Aerosols and Clouds: Laboratory Studies. *Atmos. Environ.* 44: 2658–2664.

Poschl, U. (2005). Atmospheric Aerosols: Composition, Transformation, Climate and Health Effects. *Angew. Chem. Int. Ed.* 44: 7520–7540.

Reid, J.S., Eck, T.F., Christopher, S.A., Koppmann, R., Dubovik, O., Eleuterio, D.P., Holben, B.N., Reid, E.A. and Zhang, J. (2005). A Review of Biomass Burning Emissions Part III: Intensive Optical Properties of Biomass Burning Particles. *Atmos. Chem. Phys.* 5: 827–849.

Romero, F. and Oehme, M. (2005). Organosulfates – A New Component of Humic-Like Substances in Atmospheric Aerosols? *J. Atmos. Chem.* 52: 283–294.

San Francisco Bay Area Air Quality Management District AirNow Santa Rosa Hourly Data Archive. ftp.airnow api.org.

Stafford, B. (2013). Pysolar Python Library, http://pyso lar.org/.

Surratt, J.D., Gomez-Gonzalez, Y., Chan, A.W.H., Vermeylen, R., Shahgholi, M., Kleindienst, T.E., Edney, E.O., Offenberg, J.H., Lewandowski, M., Jaoui, M., Maenhaut, W., Claeys, M., Flagan, R.C. and Seinfeld, J.H. (2008). Organosulfate Formation in Biogenic Secondary Organic Aerosol. *J. Phys. Chem. A* 112: 8345–8378.

U.S. Census Bureau (2010). Census 2010 Demographic Profile.

Ziemke, J., Chandra, S., Duncan, B., Froidevaux, L., Bhartia, P., Levelt, P. and Waters, J. (2006). Tropospheric Ozone Determined from Aura OMI and MLS: Evaluation of Measurements and Comparison with the Global Modeling Initiative's Chemical Transport Model. *J. Geophys. Res.* 111: D19303.

*Received for review, February 11, 2015*
*Revised, July 13, 2015*
*Accepted, August 11, 2015*